Published in final edited form as:
Anat Rec (Hoboken). 2013 April ; 296(4): . doi:10.1002/ar.22675.

MACROPHAGES ARE UNSUCCESSFUL IN CLEARING AGGREGATED ALPHA-SYNUCLEIN FROM THE GASTROINTESTINAL TRACT OF HEALTHY AGED FISCHER 344 RATS

Robert J. Phillips[*], **Cherie N. Billingsley**, and **Terry L. Powley**
Purdue University, Department of Psychological Sciences, West Lafayette, IN 47907-2081

Abstract

With age, alpha-synuclein (α-SYNC) misfolds and forms insoluble deposits of protein in the myenteric plexus, leading presumably to dystrophy and degeneration in the circuitry controlling gastrointestinal (GI) function. The present experiment examined aggregates of α-SYNC in the aging small intestine and investigated how macrophages in the wall of the GI tract respond to these aberrant deposits. Groups of adult and aged Fisher 344 rats were studied. Whole mounts of duodenal, jejunal and ileal smooth muscle wall, including the myenteric plexus, were prepared. Double labeling immunohistochemistry was used to stain α-SYNC protein and the phenotypic macrophage antigens CD163 and MHCII. Alpha-synuclein accumulated in dense aggregates in axons of both postganglionic and preganglionic neurons throughout the small intestine. Staining patterns suggested that deposits of protein occur initially in axonal terminals and then spread retrogradely towards the somata. Macrophages that were adjacent to dystrophic terminal processes were swollen and contained vacuoles filled with insoluble α-SYNC, and these macrophages commonly had the phenotype of alternatively activated phagocytes. The present results suggest that macrophages play an active phagocytotic role in removing α-SYNC aggregates that accumulate with age in the neural circuitry of the gut. Our observations further indicate that this housekeeping response does not clear the protein sufficiently to eliminate all synucleinopathies or their precursor aggregates from the healthy aging GI tract. Thus, accumulating deposits of insoluble α-SYNC in the wall of the GI tract may contribute, especially when compounded by disease or inflammation, to the age-associated neuropathies in the gut that compromise GI function.

Keywords

Aging; Enteric; Myenteric; Resident Macrophage

Introduction

Across the lifespan, extensive degenerative and regenerative changes occur in the enteric nervous system (ENS) of the gut. These changes include death of significant numbers of neurons and supporting glial cells (Santer and Baker, 1988; Gabella, 1989; Phillips and Powley, 2001, 2007; Phillips et al., 2003, 2004), loss of a substantial amount of visceral afferent and sympathetic motor innervation (Baker and Santer, 1988; Phillips et al., 2006, 2010), increase in the density of surviving nerve fiber endings (Belai et al., 1995; Kasparek

[*]Corresponding Author: Robert J. Phillips, Purdue University, Department of Psychological Sciences, 703 Third Street, West Lafayette, IN 47907-2081, Telephone: 765-494-6268, Fax: 765-496-1264, rphillip@psych.purdue.edu.

et al., 2009), modifications in synaptic efficacy (Giaroni et al., 1999; Vasina et al., 2006), and accumulation of aggregates of misfolded proteins (Wakabayashi et al., 1990; Wakabayashi and Takahashi, 1997; Braak et al., 2006; Phillips and Powley, 2007; Phillips et al., 2008, 2009; Pouclet et al., 2012).

The protein alpha-synuclein (α-SYNC) is widely expressed in the autonomic innervation of the gastrointestinal (GI) tract (Phillips et al., 2008; Pouclet et al., 2012), and with age, dense aggregates of α-SYNC progressively accumulate in both the intrinsic and extrinsic elements of the ENS (Wakabayashi et al., 1990; Braak et al., 2006; Phillips et al., 2009). Indeed, the presence in the ENS of inclusions and debris immunoreactive for α-SYNC may explain in part incidences of debilitating digestive symptoms in otherwise healthy elderly individuals (Talley et al., 1992; Majumdar et al., 1997; Jellinger, 2011; Pfeiffer, 2011; Pouclet et al., 2012) as well as age-associated degenerative processes such as Parkinson's disease (Braak et al., 2006; Derkinderen et al., 2011).

The accumulation of aggregated α-SYNC in the aging gut emphasizes the need to understand the mechanisms that normally dispose of deposits of insoluble α-SYNC and other cellular debris in the gut (Sato et al., 2007). One key candidate mechanism is phagocytosis by macrophages (Bain and Mowat, 2011; Liddiard et al., 2011; Smith et al., 2011). Macrophages are typically categorized either as a*lternatively activated* macrophages that use phagocytosis as their primary housekeeping strategy (Ryter, 1985; Gordon, 2003), or as *classically activated* macrophages that use phagocytosis as a key defense against exogenous pathogens (Mege et al., 2011; Mosser, 2003; Varin & Gordon, 2009).

We recently reported that macrophages are in close association with aggregated α-SYNC in the smooth muscle wall of the aged GI tract (Phillips and Powley, 2012), and speculated that the presence of misfolded proteins in dystrophic neurons or the extracellular space may mobilize the local resident macrophage population to clear out the debris. Such a proposed process would be analogous, for example, to that of microglia, which are efficient scavengers of aggregated proteins (Neumann et al., 2009), and consistent with Zhang and colleagues (2005) observation that microglia are activated by the addition of "aged" α-SYNC to the medium of a microglia-enriched culture. Taking this analogy further, it is informative that CNS macrophages, i.e. microglia, partially lose effectiveness with age (Streit, 2006), and the sustained production of extracellular α-SYNC aggregates in the CNS progressively outpaces the disposal of aggregates (Dheen et al., 2007; Miller & Streit, 2007). A similar process in the aging gut would predict that progressive accumulation of aggregated α-SYNC would result in less efficient removal by macrophages. Thus, characterizing both the accumulation of α-SYNC deposits in the ENS and the putative phagocytotic responses of macrophages neighboring the protein aggregates could be essential to achieving an understanding of the phenomena of age-related cell death and degenerative changes in the nervous innervation of the GI tract (Phillips and Powley, 2001, 2007; Phillips et al., 2010).

The goals of the present study, therefore, were to 1) characterize the morphology of macrophages in the wall of the GI tract of aged rodents along with providing quantitative descriptions of the distribution patterns of the macrophages, 2) evaluate macrophages in relation to dystrophic neuronal processes and endings and aggregated protein immunoreactive for α-SYNC, and 3) ascertain if macrophages display phagocytotic responses to α-SYNC inclusions.

Methods

Subjects

Virgin male Fischer 344 (F344; n = 24) rats were purchased, at the ages sampled, from the National Institute on Aging colony maintained by Taconic Farms (Germantown, NY). Adult (5–10 months of age; n = 8) and aged (24 months of age; n = 12) rats were used. The various staining protocols (e.g., primary dilution curves, primary sequence, chromogen intensity, etc) were initially determined in a less costly cohort of young-adult rats (3 months of age; n = 4) from which whole mounts were also examined. Rats were group housed (n=2/cage) in polypropylene cages containing sterilized Alpha-dri bedding (Shepherd Specialty Papers; Cincinnati Lab Supply, Cincinnati, OH) in a room kept at 22–24°C on a 12:12 hour light:dark schedule. Solid chow (NIH-31M; Zeigler, Gardners, PA) and tap water were available ad libitum. Conditions in the AAALAC-approved colony approximated the housing, husbandry, and barrier conditions at Taconic Farms, but did not provide a specific pathogen-free environment. All procedures were conducted in accordance with the National Institute of Health *Guide for the Care and Use of Laboratory Animals* (NIH Publications No. 80-23) revised 1996, and approved by the Purdue University Animal Care and Use Committee. Every effort was made to minimize the number of rats used and their suffering.

Fixation Protocol and Tissue Samples

Rats were weighed, killed with a lethal dose of sodium pentobarbital (180 mg/kg, i.p.), and perfused through the left ventricle of the heart with 200 ml of 0.01 M PBS followed by 400 ml of Zamboni's fixative. The small intestine was sampled. Intestinal whole mounts consisted of two 3 cm segments from the duodenum (the first 6 cm anal to the pyloric sphincter), jejunum (typically the middle third), and ileum (the first 6 cm oral to the ileocaecal junction). Whole mounts were fixed overnight in the same fixative, and then the mucosa, submucosa, and circular muscle were removed, producing specimens consisting of the longitudinal muscle layer and myenteric plexus.

Permanent Immunohistochemistry

Permanent double labeling protocols were used to label α-SYNC protein and macrophages in the same specimens. In the case of macrophage labeling, two antibodies were used--individually, in separate series--to evaluate the phenotypic characteristics of macrophages, because of the quality as well as the relative completeness of the labeling they yield. Specifically, antibodies to CD163 and MHCII were used. The CD163 antibody selectively recognizes the membrane glycoprotein receptor CD163 (also known as ED2) in macrophages that functions as a bacterial receptor (Fabriek et al., 2009). CD163 is expressed by resident macrophages as well as by activated and alternatively activated macrophages (Kalff et al., 1998). The MHCII antibody recognizes a monomorphic determinant of the rat 1-A antigen found in antigen-presenting cells, including macrophages. MHCII is not regularly expressed in resident macrophages, but is expressed in activated macrophages and in some types of alternatively activated macrophages (Mikkelsen et al., 2011).

For a more detailed description of the labeling protocol and primaries used, see Phillips and Powley (2012). Briefly, double immunoperoxidase staining of free-floating whole mounts consisted of the following sequential steps: 6×5-min rinses in 0.1 M phosphate-buffered saline (PBS; pH 7.4); 30-min soak in methanol:H_2O_2 (4:1) to inhibit endogenous peroxidase activity; 6×5-min rinses in PBS; 4-d soak in normal serum block (0.5% Triton X-100, 5% normal horse serum, 2% bovine serum albumin, and 0.08% Na Azide in PBS); 24-h soak in mouse anti-rat synuclein-1 (α-SYNC; 1:5000; 610787; BD Transduction, San Jose, CA) in primary diluent (0.3% Triton X-100, 2% normal horse serum, 2% BSA, and 0.08% Na Azide in PBS); 6×5-min rinses in PBST (PBS + 0.3% Triton X-100); 2-h soak in

biotinylated anti-mouse IgG, rat absorbed, raised in horse (1:500; BA-2001; Vector Laboratories, Inc., Burlingame, CA) in secondary diluent (0.3% Triton X-100, 2% normal horse serum, and 2% bovine serum albumin in PBS); 6×5-min rinses in PBS; 1-h incubation in ABC (PK-6100; Vector laboratories) in PBS; 6×5-min rinses in PBS; 3-min reaction with DAB and H_2O_2 in tris buffered saline; 3×5-min rinses in cold dH_2O; 3×5-min rinses in PBS; overnight incubation in normal serum block; 15-min Avidin block; 3×5-min rinses in PBS; 15-min Biotin block; 3×5-min rinses in PBS; 24-h soak in either mouse anti-rat CD163 (1:1000; MCA342R; AbD Serotec, Oxford, UK) or mouse anti-rat major histocompatibility complex class II (1:4000; MCA46R; AbD Serotec) in primary diluent; 6×5-min rinses in PBST; 2-h soak in biotinylated anti-mouse IgG, rat absorbed, raised in horse (1:500; Vector Laboratories, Inc.) in secondary diluent, 6×5-min rinses in PBS; 1-h incubation in ABC in PBS; 6×5-min rinses in PBS; 5-min reaction with Vector SG Peroxidase Substrate Kit (SK-4700; Vector Laboratories, Inc.) in PBS (working solution mixed according to the manufacturer's instructions immediately prior to use); and finally, 6×5-min rinses in cold dH_2O to stop the substrate reaction. Every step was done at room temperature with gentle agitation on a shaker table. Specificity of the staining was determined by omitting the primary antibody in randomly chosen whole mounts from regions of the small intestine not used for the study. Stained tissue segments were mounted on gelatin-coated slides, air-dried overnight, dehydrated in an ascending series of alcohols, cleared in two xylene steps, and coverslipped with Cytoseal XYL (Richard-Allen Scientific, Kalamazoo, MI).

Whole Mount Reconstructions

Ultra-high resolution digital "mosaics" of intestinal whole mounts were generated using a Leica DM5500B (Leica Microsystems Inc., Buffalo Grove, IL) automated upright microscope running Surveyor with Turboscan (V. 6.0.1.4; Objective Imaging, Cambridge, UK). These mosaics are wide-field composites of adjacent micrographs, in x- and y- from a single z-plane, which are aligned and merged by the software. As with individual photomicrographs, mosaics from different focal planes can also be combined as z-stacks and merged into all-in-focus composites using the software and then visually scanned using Surveyor Viewer (OIViewer Application, V5.5.5.18; Objective Imaging). Such mosaics aided in understanding the relationships between microscopic features and the overall structure of the whole mount specimens (cf., Panels A in Figures 7 and 8). Specifically, in the case of the present study, the mosaics provided a means of identifying dystrophic α-SYNC axons and aggregates of α-SYNC protein and determining their relationship to resident macrophages.

Distribution of Macrophages

Stereo Investigator (V.10; MicroBrightField, Inc., Williston, VT) was used for random unbiased selection of sites sampled in whole mounts stained for either CD163+ or MHCII+ resident macrophage. Briefly, the contour of a whole mount was traced, and then 25 to 50 sites within the contour were chosen using the fractionator probe. A square 0.5 mm × 0.5 mm grid was projected onto each of the sites and every macrophage that fell within a grid was marked. In this way, both the mesenteric attachment and the antimesenteric aspect of the tissue were sampled. Observations were done at a magnification of 250x by the same experimenter (CNB), who was blind to the age of the rat from which the whole mount originated. Contours and 3D surface maps of the distribution of the macrophages were generated using a grid-based graphics program (Surfer 10, V10.4.799; Golden Software, Inc., Golden, CO).

Tracings of Macrophages and Neural Elements

Low-magnification images that encompass the whole cell of macrophages are particularly useful in evaluating the status of cells. In such images, however, it is often difficult to see

(particularly in double-stained whole mounts) the finest, lightly stained details such as filopodia. As needed to evaluate such low-contrast elements (e.g., fine tendrils and nodules extending from the main processes), images of the macrophages and neural elements were captured (see paragraph below for descriptions of imaging and focus stacking) using high power objectives (e.g., 63x oil or 100x oil objectives), opened in Photoshop CS5 (Adobe Systems, San Jose, CA) on a Wacom Tablet (DTU-2231, 21.5″ Interactive Pen Display, full high definition resolution, 1920×1080; Wacom, Vancouver, WA), enlarged 300–500%, and then traced as high contrast silhouettes onto a transparent overlay using the pen tool and function. The accuracy of the silhouettes was validated during and after the tracing process using the transparency slider to compare the final tracing to each individual plane of focus throughout the entire stack of images comprising the extended depth of field. This process ensured that the final silhouette represented accurately and in their entirety the finer details of the macrophage morphology. Tracings of the macrophages were then reduced or enlarged to the desired magnification without loss in resolution.

Brightfield Image Capture, Image Evaluation, and Image Post-processing

Brightfield photomicrographs were acquired using a Leica DM (Leica Microsystems Inc.) microscope fitted with a Spot Flex camera that was controlled using Spot Software (V4.7 Advanced Plus; Diagnostic Instruments, Sterling Heights, MI). To assess the spatial relationships of cells and neurites, images were evaluated both in “z-stacks” and in single-image planes. Focus stacking (Gulbins and Gulbins, 2009) was used to maximize the depth of field of images taken from thick GI whole mounts. Specifically, by merging a series of shots taken at different focal distances along the z-axis with overlapping regions of focus, single all-in-focus images containing the elements of interest were generated using Helicon Focus Pro X64 (Version 5.1.23; HeliconSoft Ltd., Kharkov, Ukraine).

To evaluate whether any candidate appositions between cells or between cells and neurites as well as any apparent inclusions within macrophages occurred in the same x- and y- plane, the putative appositions or inclusions were evaluated by focusing single-plane-by-single-plane through the z-stacks. For all illustrations, all-in-focus images are clearly stated as such in the appropriate figure legend(s); otherwise, the image represents a single plane of focus.

Photoshop CS5 (Adobe Systems) was used to: (1) organize the layout of the figures; (2) adjust color, hue, brightness, contrast, and sharpness of images; and (3) apply text and scale bars. The goal of these adjustments was to generate final images which accurately conveyed our observations on the nervous innervation of the GI tract.

Results

Morphology and Distribution

The double labeling protocol and specific antibodies used in the present survey made it practical to identify α-SYNC+ neurons and processes and determine their organization and distributions as well as to recognize different macrophage phenotypes and their responses to aggregated α-SYNC. In brief, the α-SYNC antibody effectively labeled neuronal somata expressing the protein (Fig. 1A) and their neurites in which the protein was transported (Fig. 1B). In addition, the a-SYNC antibody labeled aggregates of the protein in swellings and varicosities of dystrophic nerve fibers (Fig. 1C), making it possible to examine accumulations of α-SYNC with age and to evaluate macrophage responses to neurons evincing synucleinopathies.

Similarly, the use of the antibodies to the two different macrophage proteins made it feasible to evaluate macrophage activational status (Fig. 2) as well as location. The CD163 antibody delineated macrophages by labeling the membrane and cytoplasm, including the cytoplasm

extending into the processes, of the phagocytes (Fig. 1C). Thus, CD163 made it possible to recognize *resident* macrophages on the basis of their relatively filopodia-free smooth-surfaced somata and their characteristic regular and semi-equidistant spacing of individual cells (Fig. 1D). The MHCII antibody also strongly labeled membrane and cytoplasm, specifically of those phagocytes displaying evidence of one or another of the activated states (Fig. 1E). Thus, the MHCII antibodies (as well as CD163 antibodies) labeled *alternatively activated* macrophages that issued filopodia, filaments, or spines (Fig. 1E, F) and that seemed less regularly distributed than resident macrophages (Fig. 2C, D). The MHCII antibody was also particularly effective in labeling macrophages with features of a *classically activated* phenotype (Fig. 1F), including those that occurred in regions with large clusters of MHCII+ monocytes (Fig. 2D). Additionally, in some cases, MHCII+ macrophages lost their morphological integrity (i.e., were no longer identifiable as either bipolar or stellate cells) as they clumped together into large masses [Fig. 2E, F; cf. the vertically oriented strings of amassed macrophages in the middle of both 2E and 2F. At higher magnifications, these agglomerations consisted of macrophages with poorly delineated somatic and nuclear boundaries.].

Alpha-Synuclein (α-SYNC) in ENS Neurites Accumulated with Age

A subpopulation of myenteric neurons was immunoreactive for α-SYNC, with the protein expressed in the cytoplasm as well as the nucleus (Fig. 1A). In the connectives, particularly the connectives of young and adult animals, axons immunoreactive for α-SYNC were smooth in appearance, but, within the ganglia, they were dotted with numerous small swellings or varicosities, presumptive synaptic contacts, as they encircled both α-SYNC+ and α-SYNC− neurons (Fig. 1B). In contrast, in the aged rats, protein aggregates intensely stained for α-SYNC had unstained or lightly stained central cores and/or inclusions (Fig. 1C).

In the whole mounts from adult rats almost all α-SYNC positive somata and fibers were normal in appearance, and there were very few incidences of either α-SYNC+ markedly swollen axons or large aggregates of α-SYNC observed. Specifically, the number of inclusions in the duodenum and jejunum of adult rats ranged from 0 to 1 per whole mount with a mean of 0.33 and 0.40 per whole mount, respectively. In aged rats, by comparison, markedly swollen axons and aggregates immunoreactive for α-SYNC were significantly more common in both the duodenum and jejunum (Unpaired t-tests; p values = 0.02 and 0.03, respectively), and ranged from 7 to 52 per duodenal whole mount and 0 to 13 per jejunal whole mount with a mean of 26 and 3.8 per whole mount, respectively. In general, in most aged rats, markedly swollen axons with dilated varicosities and dystrophic neurites positive for α-SYNC were observed throughout the entire length of the small intestine (Fig. 3), however it is important to note that in some cases we observed some whole mounts sampled from an aged rat that had no apparent accumulation of aggregated α-SYNC.

The terminal fields of the α-SYNC+ markedly swollen axons were traced (see Fig. 3D for example of a typical tracing) to better characterize the dystrophic endings expressing the protein. Such dystrophic endings in the terminal fields were densely populated with swollen axons and aggregates intensely immunoreactive for α-SYNC (Fig. 3A, B). By tracing back along the fibers that formed these large dystrophic and possibly degenerating terminal fields, it was practical to follow the different neurites back to axons that no longer branched, i.e. presumably to the parent axons from which the terminal arbors originated. Using this strategy, we determined that, typically, the parent axons were themselves not yet degenerating or accumulating deposits of α-SYNC (Fig. 3C, D). The parent axons were, however, often swollen many times larger in diameter compared to adjacent healthy or typical looking α-SYNC+ axons.

Phagocytosis of Aggregated Alpha-synuclein by Macrophages

At sites with deposits of aggregated α-SYNC in the myenteric connectives and the muscle wall, the local macrophages adjacent to the sites had transformed into phagocytes (Fig. 4 and Fig. 5). Evidence of phagocytosis was the presence of large inclusions of α-SYNC located within the cytoplasm of macrophages (Fig. 4H, Fig. 5B–D, G and Fig. 6). The internalized debris ranged from large, intensely stained aggregates with well delineated borders to diffuse, weakly stained formations that typically filled the vacuole-like structures within the cytoplasm of the phagocyte (Fig. 4H, Fig. 5 and Fig. 6). Many of the phagocytotic macrophages that contained partially degraded remains of α-SYNC+ debris exhibited the broken and fragmented somatic silhouettes commonly associated with dissolution and possibly cell death (Fig. 6).

Alpha-Synuclein Immunoreactive Inclusions in Relation to Macrophage “Hot Spots”

Estimates of the overall distributions of CD163+ cells did not reveal significant differences in cell number between the adult and aged rats for either the duodenum or jejunum (Unpaired t-tests; p values > 0.05 for both regions). The mean ± SEM of cells/0.25 mm^2 for adult and aged rats in the duodenum was 66.8 ± 3 and 69.5 ± 5 and for the jejunum 48.8 ± 2 and 45.0 ± 2, respectively.

Whereas the means of the overall counts of the CD163+ macrophages did not indicate an effect of age, our surveys of the mosaics of the whole mounts revealed foci or local sites where macrophages appeared to be more classically activated and had infiltrated en mass into “hot spots” (Fig. 7).

Qualitative observations of both the macrophage “hot spots” and sites occupied by α-SYNC + aggregates and swollen terminal fields suggested that the hot spots were independent of the terminal fields with aggregates of α-SYNC, so we undertook a more systematic analysis of this apparent independence. To evaluate whether the “hot spots” occurred at the sites of α-SYNC aggregates, the locations of α-SYNC+ aggregates and swollen terminals along with macrophage hot spots were mapped for the same whole mounts. Specifically, the macrophage counts were overlaid on to their respective mosaic areas in the whole mounts, where there was an increased density of cells (Fig. 7A, D). Examination of these “hot spots” of activated macrophages at higher magnification revealed that neither α-SYNC+ markedly swollen axons nor large aggregates of α-SYNC were present at these sites in the mosaics (Fig. 7B, C). Conversely, at sites where large aggregates of α-SYNC or α-SYNC+ markedly swollen axons (Fig. 8) were present there was no change in the density of the macrophages; specifically, there were no hot spots or dense clumps of the macrophages at the aggregated α-SYNC sites (Fig. 8B, C). This pattern was consistent throughout the small intestine (Fig. 3).

Age-related Accumulation of Aggregated α-SYNC in Varicosities Contacting Myenteric Somata

Small axonal varicosities immunoreactive for α-SYNC were also present within the ganglia of the myenteric plexus (Fig. 1B, Fig. 9A). The varicosities were typically scattered throughout the ganglia, but they also frequently formed ring-like structures (Fig. 9A). These ring-like structures were presumably preganglionic or intrinsic efferent projections to myenteric neurons insofar as the α-SYNC+ varicosities delineated perimeters of what were apparently unlabeled neurons within the ganglion (i.e., α-SYNC− neurons). [Small α-SYNC + varicosities also formed terminal rings around α-SYNC+ neurons, but, in such cases, the presence of the same antibody labeling both the varicosities and the somata made it difficult to distinguish the separate structures for routine assessment.]

In young and adult rats, the varicosities were small and intensely stained for α-SYNC, and individually distinct, based on spacing with minimal overlap. Some of these ring-like structures became more pronounced with age as a result of an increase in the number of α-SYNC+ varicosities present around the perimeter of the unstained neurons (Fig. 9A, B) and/or the presence of aggregated α-SYNC (Fig. 9C). In aged rats, the varicosities of some of these ring-like structures were replaced by large aggregates or fused deposits of α-SYNC to such a degree that the individual varicosities, which made up the ring-like structures in adult rats, were no longer individually distinguishable (Fig. 9D–F).

Macrophages also Target Myenteric Neurons

The layer of the muscularis containing the myenteric plexus was heavily infiltrated by macrophages. Macrophage cells were present in close proximity to the ganglia and connectives, and most ganglia were effectively outlined by macrophages (Fig. 10A). Macrophages stationed around the perimeter of the ganglia often--and particularly in adult animals--did not make contact with the neurons and neurites within the ganglion. When the macrophages did infiltrate the ganglion, however, the process varied from subtle forays into the plexus to aggressive invasions across the plexus boundaries (Fig. 10B). In the more subtle cases, the soma of the macrophage would remain outside of the plexus while its processes would extend into the plexus, making contact with either the soma, dendrite, or axon of a neuron (Fig. 10A); whereas the more aggressive breach of the ganglion's perimeter consisted of the soma of the macrophage migrating to the center of the ganglion and spreading its processes throughout the entire cluster of neurons (Fig. 10B).

In whole mounts from adult rats, macrophages within the vicinity of terminal ring-like structures typically silhouetted the ganglia within which the ring of varicosities was located (Fig. 9A). In contrast, in the case of aged animals, where the preganglionic (or intrinsic efferent) terminal rings consisted of dense aggregates of α-SYNC, the macrophages would often have infiltrated the ganglia and made contact with the protein inclusions (Fig. 9D–F).

In the myenteric plexus of aged rats, some α-SYNC+ neurons were embraced by the processes of activated macrophages expressing MHCII (Fig. 10C–E). These macrophages had unusual phenotypes, with their processes covering the entire circumferences of the contacted α-SYNC+ neurons and spreading further throughout the ganglion to contact other α-SYNC+ and α-SYNC− neurons (Fig. 10C). Often, in aged animals, ganglia were infiltrated by numerous macrophage cells (Fig. 10F, G), and, in such instances, monocytes were similarly observed clustered within the vicinity of the ganglion (Fig. 10C, F).

Discussion

The present results provide new information on (a) the pattern of α-SYNC accumulation in the autonomic projections to the duodenum, jejunum and ileum with aging, (b) how such accumulations apparently begin distally in or near neural terminal varicosities and progressively affect more proximal segments of neurites, (c) how alternatively activated macrophages use phagocytosis--but not classical inflammatory responses--to clear, albeit incompletely, deposits of α-SYNC, and (d) the way that, with aging, a second type of macrophage response involving classical activation in the intestine occurs at local sites or foci of inflammation that do not involve deposits of α-SYNC. The results can be discussed in terms of these new observations.

Alpha-Synuclein Accumulates within the Aged ENS

A plausible hypothesis is that the synucleinopathies in the duodenum, jejunum and ileum observed in the present study contribute to the losses of enteric neurons (Gabella, 1989;

Phillips & Powley, 2001; Phillips et al., 2003) and sympathetic motor innervation (Baker & Santer, 1988; Phillips et al., 2006) that have been documented in the same elements of the autonomic circuitry in the same regions of the (presumably "normal" or "healthy") aging GI tract. Similarly the synucleinopathies could be potentially analogous to the widespread pathology described in the spinal and autonomic nervous system (Bloch et al., 2006), and the midbrain and limbic cortex of asymptomatic "healthy" elderly subjects (Jellinger, 2004, 2009).

The present observations not only support the hypothesis that deposition of α-SYNC in autonomic circuitry may be one of the mechanisms whereby aging-associated wear and tear induces dystrophic changes in the ENS, they also suggest the possibility that the aggregation of α-SYNC may result from macrophage housekeeping functions progressively slowing with age and failing to remove sufficient misfolded protein to protect neurons that express α-SYNC.

Additionally, our results indicate that "hot spots" of infiltrating activated macrophages do occur in the muscle wall of the aging small intestine, and that these focal sites of inflammation are not the loci in which the α-SYNC+ dystrophic neural processes are eliciting local macrophagic phagocytotic debris removal. Though the present observations cannot establish whether the macrophages with classically activated phenotypes are responding to local pathogen invasions or ischemic complications or other insults, the results do suggest that the macrophage hot spots in the intestinal wall are independent of the synucleinopathies of ENS aging, and more likely associated with aging and the other progressive disorders of the GI tract that reflect wear and tear on the gut and that accumulate over the lifespan.

Alpha-Synuclein Aggregation in ENS Begins in Nerve Terminals

A notable observation in the present survey is the fact that aggregated α-SYNC deposits appear to develop initially in the distal terminals of the postganglionic and preganglionic projections in the gut, a pattern similar to that previously reported for the autonomic innervation of the heart (Orimo et al., 2008), and recently reported for nigral dopamine neurons in the striatum (Lundblad et al., 2012). In particular, with age, the most distal segments of axons projecting in the muscle wall and tertiary plexus (i.e., postganglionic or sympathetic efferents) evinced terminal swellings and dilations filled with dense α-SYNC deposits. Similarly, varicosities (i.e. presumptive terminals, including some which would be vagal--see ref. Phillips et al., 2008--and others which would be intrinsic) encircling myenteric neurons became swollen and enlarged with deposits of α-SYNC. The axons of all neurons containing aggregates of α-SYNC conformed to this pattern. In addition, a subset of those neurons with terminal deposits of the protein also contained aggregates of α-SYNC more proximally in the axons. Together the two patterns (i.e., protein in just terminals or protein in terminals plus more proximal axon) suggest that the synucleiopathies may be initiated in the terminals and then later spread retrogradely in the axon.

These axonal synucleinopathies in the GI tract had characteristics of Lewy neurites, but some reservations need to be noted. First, the structural material we describe as "aggregates" or "deposits" of "misfolded" and "insoluble" α-SYNC were evaluated only by immunohistochemical and morphological criteria. In particular, the aggregated protein was seen in grossly dilated, distorted, and dystrophic terminals and neurites. We did not, however, perform a series of digestion assays to determine the extent to which the proteinaceous material could be solublized. Second, we have provisionally concluded that the α-SYNC masses in terminals and neurites distort neuronal structure and function, thus producing neuropathies, but we cannot rule out the possibility that the neuronal dystrophies preceded the accumulation of the protein. Third, the criteria for Lewy neurites and Lewy

bodies have been the subject of extensive discussion, of course, and it is unclear whether a fuller examination of the neurites with intra-axonal deposits of α-SYNC will satisfy all candidate criteria for Lewy neurites. Nonetheless, the axonal synucleinopathies in the GI tract do (1) consist of α-SYNC, (2) express hyperphosphorylated tau protein as well as α-SYNC (Phillips et a., 2009), and (3) contain lightly stained central cores and/or inclusions. Furthermore, previous work has recognized the axonal synucleinopathies in the gut as Lewy neurites (Braak et al., 2006; Cersosimo and Benarroch, 2008; Lebouvier et al., 2009; Pouclet et al., 2012).

The pattern of α-SYNC deposition in autonomic projections suggests conclusions about how, as well as where, the misfolding that is responsible for α-SYNC aggregation in the innervation of the gut is concentrated. Staining of soluble α-SYNC material is observed in the neuronal somata (the protein is generally assumed to be transported into the axon once it is manufactured in the soma, and different antibodies have been shown to detect the protein in neuronal somata [Maroteaux et al., 1988; Andringa et al., 2003; Yu et al., 2007]), axons and varicosities. The fact that the protein typically aggregates in dense insoluble deposits in varicosities and terminal segments of axons raises the possibility that its participation in signaling events in presynaptic terminals may prime the molecule for misfolding. Such an inference would be consistent with either a hypothesis suggesting that events associated with intracellular trafficking in the presynaptic terminal could expose the protein to misfolding events or a hypothesis that material captured from the synaptic cleft by reuptake and endocytosis and then incorporated into presynaptic processes might induce misfolding of the susceptible protein (Desplats et al., 2009). Such a mechanism might also explain how a basal level of synucleinopathy seen in normal or “healthy” aging might be exaggerated by pathogens. With the burden of increasing deposits of α-SYNC seen in normal aging, the autonomic circuitry might lose resilience and become more vulnerable to additional challenges that compound the misfolding of the protein or favor the incorporation of pathogens.

Gut Macrophages Engulf α-SYNC by Phagocytosis

One of the questions addressed by the present experiment is whether aggregated α-SYNC in the ENS is cleared or removed by macrophages through the mechanism of phagocytosis. Such a process has been observed for brain microglia, i.e. CNS macrophages (Park et al., 2008), but it is unknown whether similar processing occurs in the gut for α-SYNC. The current observations clearly suggest that such a mechanism does in fact operate in the GI tract. Importantly, too, the present observations document that with normal aging the protein continues to accumulate in dystrophic neurites, indicating that the phagocytotic response of local macrophages is insufficient to prevent the accumulation of ENS synucleinopathies over the lifespan.

Such a progressive accumulation of α-SYNC with age might result from different mechanisms which, of course, are not mutually exclusive: Conceivably, the base rate of protein aggregation may modestly but consistently outpace phagocytosis and other housekeeping operations throughout the lifespan, leading to steady and incremental accumulation. It is also possible that the aging ENS actually produces a more resistant or insoluble misfolded protein than does the young or adult ENS. Alternatively, aspects of the aging process may compromise macrophage function, leading to an accelerating accumulation of insoluble protein as phagocytotic processes diminish. Indeed, there is evidence that macrophages do lose efficacy with age (Streit, 2006; Miller & Streit, 2007).

The pattern of macrophagic responses to dystrophic α-SYNC+ neurites also provides another perspective on the way the protein accumulates with age. The present results indicate that aggregates of the protein appear to elicit a phagocytotic response from those

macrophages immediately neighboring the dystrophic neural elements. This response appears to be a limited housekeeping response of alternatively activated macrophages responding to the local neuropathy. Though macrophages can also, by the cytokine and chemokine signaling that is associated with classical activation, elaborate inflammatory responses and provoke degenerative changes (Bain and Mowat, 2011; Liddiard et al., 2011), α-SYNC aggregates in the ENS do not appear to stimulate an aggressive infiltration of macrophages or monocytes to the site, nor do they appear to produce a classical activation of macrophages (Mikkelsen, 1995; Sato et al., 2007). In this regard, the alternative activational response pattern of macrophages in the wall of the gut to α-SYNC accumulation is much like the partial activation response pattern expressed by macrophages in the gut lamina propria to local disturbances (Bain and Mowatt, 2011). Apparently, in the case of α-SYNC, any cytokine and/or chemokine signaling associated with deposition of the insoluble form of the protein and the phagocytosis it elicits do not fully mobilize innate immune system responses. An interesting corollary of such a conclusion is that treatments designed to mobilize more robust macrophage housekeeping responses to α-SYNC aggregates might be a strategy for limiting the gut synucleinopathies of normal aging.

Acknowledgments

We are grateful to E. Lydster, F. Martin, M. McCarthy, and B. Ringer for help with the processing and preparation of the tissue for microscopy; to J. Gilbert for help with photography; and to J. McAdams for proofreading versions of the manuscript. This work was supported by grants from the National Institute of Diabetes and Digestive and Kidney Diseases (NIH DK61317 and DK27627).

Literature Cited

Andringa G, Du F, Chase TN, Bennett MC. Mapping of rat brain using the Synuclein-1 monoclonal antibody reveals somatodendritic expression of alpha-synuclein in populations of neurons homologous to those vulnerable to Lewy body formation in human synucleopathies. J Neuropathol Exp Neurol. 2003; 62:1060–1075. [PubMed: 14575241]

Bain CC, Mowat AM. Intestinal macrophages - specialised adaptation to a unique environment. Eur J Immunol. 2011; 41:2494–2498. [PubMed: 21952804]

Baker DM, Santer RM. A quantitative study of the effects of age on the noradrenergic innervation of Auerbach's plexus in the rat. Mech Ageing Dev. 1988; 42:147–158. [PubMed: 3361967]

Belai A, Cooper S, Burnstock G. Effect of age on NADPH-diaphorase-containing myenteric neurones of rat ileum and proximal colon. Cell Tissue Res. 1995; 279:379–383. [PubMed: 7895275]

Bloch A, Probst A, Bissig H, Adams H, Tolnay M. Alpha-synuclein pathology of the spinal and peripheral autonomic nervous system in neurologically unimpaired elderly subjects. Neuropathol Appl Neurobiol. 2006; 32:284–295. [PubMed: 16640647]

Braak H, de Vos RA, Bohl J, Del Tredici K. Gastric alpha-synuclein immunoreactive inclusions in Meissner's and Auerbach's plexuses in cases staged for Parkinson's disease-related brain pathology. Neurosci Lett. 2006; 396:67–72. [PubMed: 16330147]

Cersosimo MG, Benarroch EE. Neural control of the gastrointestinal tract: implications for Parkinson disease. Mov Disord. 2008; 23:1065–1075. [PubMed: 18442139]

Derkinderen P, Rouaud T, Lebouvier T, Bruley des Varannes S, Neunlist M, De Giorgio R. Parkinson disease: the enteric nervous system spills its guts. Neurology. 2011; 77:1761–1767. [PubMed: 22067963]

Desplats P, Lee HJ, Bae EJ, Patrick C, Rockenstein E, Crews L, Spencer B, Masliah E, Lee SJ. Inclusion formation and neuronal cell death through neuron-to-neuron transmission of alpha-synuclein. Proc Natl Acad Sci U S A. 2009; 106:13010–13015. [PubMed: 19651612]

Dheen ST, Kaur C, Ling EA. Microglial activation and its implications in the brain diseases. Curr Med Chem. 2007; 14:1189–1197. [PubMed: 17504139]

Fabriek BO, van Bruggen R, Deng DM, Ligtenberg AJ, Nazmi K, Schornagel K, Vloet RP, Dijkstra CD, van den Berg TK. The macrophage scavenger receptor CD163 functions as an innate immune sensor for bacteria. Blood. 2009; 113:887–892. [PubMed: 18849484]

Gabella G. Fall in the number of myenteric neurons in aging guinea pigs. Gastroenterology. 1989; 96:1487–1493. [PubMed: 2714575]

Giaroni C, De Ponti F, Cosentino M, Lecchini S, Frigo G. Plasticity in the enteric nervous system. Gastroenterology. 1999; 117:1438–1458. [PubMed: 10579986]

Gordon S. Alternative activation of macrophages. Nat Rev Immunol. 2003; 3:23–35. [PubMed: 12511873]

Gulbins, J.; Gulbins, R. Photographic multishot techniques : high dynamic range, super-resolution, extended depth of field, stitching. Nook, Rocky, editor. Distributed by O'Reilly Media; Santa Barbara, CA: 2009.

Jellinger KA. Lewy body-related alpha-synucleinopathy in the aged human brain. J Neural Transm. 2004; 111:1219–1235. [PubMed: 15480835]

Jellinger KA. Formation and development of Lewy pathology: a critical update. J Neurol. 2009; 256(Suppl 3):270–279. [PubMed: 19711116]

Jellinger KA. Synuclein deposition and non-motor symptoms in Parkinson disease. J Neurol Sci. 2011; 310:107–111. [PubMed: 21570091]

Kalff JC, Schwarz NT, Walgenbach KJ, Schraut WH, Bauer AJ. Leukocytes of the intestinal muscularis: their phenotype and isolation. J Leukoc Biol. 1998; 63:683–691. [PubMed: 9620660]

Kasparek MS, Fatima J, Iqbal CW, Duenes JA, Sarr MG. Age-related changes in functional NANC innervation with VIP and substance P in the jejunum of Lewis rats. Auton Neurosci. 2009; 151:127–134. [PubMed: 19734110]

Lebouvier T, Chaumette T, Paillusson S, Duyckaerts C, Bruley des Varannes S, Neunlist M, Derkinderen P. The second brain and Parkinson's disease. Eur J Neurosci. 2009; 30:735–741. [PubMed: 19712093]

Liddiard K, Rosas M, Davies LC, Jones SA, Taylor PR. Macrophage heterogeneity and acute inflammation. Eur J Immunol. 2011; 41:2503–2508. [PubMed: 21952806]

Lundblad M, Decressac M, Mattsson B, Bjorklund A. Impaired neurotransmission caused by overexpression of alpha-synuclein in nigral dopamine neurons. Proc Natl Acad Sci. 2012; 109:3213–3219. [PubMed: 22315428]

Majumdar AP, Jaszewski R, Dubick MA. Effect of aging on the gastrointestinal tract and the pancreas. Proc Soc Exp Biol Med. 1997; 215:134–144. [PubMed: 9160041]

Maroteaux L, Campanelli JT, Scheller RH. Synuclein: a neuron-specific protein localized to the nucleus and presynaptic nerve terminal. J Neurosci. 1988; 8:2804–2815. [PubMed: 3411354]

Mege JL, Mehraj V, Capo C. Macrophage polarization and bacterial infections. Current opinion in infectious diseases. 2011; 24:230–234. [PubMed: 21311324]

Mikkelsen HB. Macrophages in the external muscle layers of mammalian intestines. Histol Histopathol. 1995; 10:719–736. [PubMed: 7579823]

Mikkelsen HB, Larsen JO, Froh P, Nguyen TH. Quantitative Assessment of Macrophages in the Muscularis Externa of Mouse Intestines. Anat Rec (Hoboken). 201110.1002/ar.21444

Miller KR, Streit WJ. The effects of aging, injury and disease on microglial function: a case for cellular senescence. Neuron Glia Biol. 2007; 3:245–253. [PubMed: 18634615]

Mosser DM. The many faces of macrophage activation. J Leukoc Biol. 2003; 73:209–212. [PubMed: 12554797]

Neumann H, Kotter MR, Franklin RJ. Debris clearance by microglia: an essential link between degeneration and regeneration. Brain. 2009; 132:288–295. [PubMed: 18567623]

Orimo S, Uchihara T, Nakamura A, Mori F, Kakita A, Wakabayashi K, Takahashi H. Axonal α-synuclein aggregates herald centripetal degeneration of cardiac sympathetic nerve in Parkinson's disease. Brain. 2008; 131:642–650. [PubMed: 18079166]

Park JY, Paik SR, Jou I, Park SM. Microglial phagocytosis is enhanced by monomeric alpha-synuclein, not aggregated alpha-synuclein: implications for Parkinson's disease. Glia. 2008; 56:1215–1223. [PubMed: 18449945]

Pfeiffer RF. Gastrointestinal dysfunction in Parkinson's disease. Parkinsonism Relat Disord. 2011; 17:10–15. [PubMed: 20829091]

Phillips RJ, Kieffer EJ, Powley TL. Aging of the myenteric plexus: neuronal loss is specific to cholinergic neurons. Auton Neurosci. 2003; 106:69–83. [PubMed: 12878075]

Phillips RJ, Kieffer EJ, Powley TL. Loss of glia and neurons in the myenteric plexus of the aged Fischer 344 rat. Anat Embryol (Berl). 2004; 209:19–30. [PubMed: 15480773]

Phillips RJ, Powley TL. As the gut ages: timetables for aging of innervation vary by organ in the Fischer 344 rat. J Comp Neurol. 2001; 434:358–377. [PubMed: 11331534]

Phillips RJ, Powley TL. Innervation of the gastrointestinal tract: patterns of aging. Auton Neurosci. 2007; 136:1–19. [PubMed: 17537681]

Phillips RJ, Powley TL. Macrophages Associated with the Intrinsic and Extrinsic Autonomic Innervation of the Rat Gastrointestinal Tract. Auton Neurosci. 2012; 169:12–27. [PubMed: 22436622]

Phillips RJ, Rhodes BS, Powley TL. Effects of age on sympathetic innervation of the myenteric plexus and gastrointestinal smooth muscle of Fischer 344 rats. Anat Embryol (Berl). 2006; 211:673–683. [PubMed: 17024301]

Phillips RJ, Walter GC, Powley TL. Age-related changes in vagal afferents innervating the gastrointestinal tract. Auton Neurosci. 2010; 153:90–98. [PubMed: 19665435]

Phillips RJ, Walter GC, Ringer BE, Higgs KM, Powley TL. Alpha-synuclein immunopositive aggregates in the myenteric plexus of the aging Fischer 344 rat. Exp Neurol. 2009; 220:109–119. [PubMed: 19664623]

Phillips RJ, Walter GC, Wilder SL, Baronowsky EA, Powley TL. Alpha-synuclein-immunopositive myenteric neurons and vagal preganglionic terminals: autonomic pathway implicated in Parkinson's disease? Neuroscience. 2008; 153:733–750. [PubMed: 18407422]

Pouclet H, Lebouvier T, Coron E, des Varannes SB, Rouaud T, Roy M, Neunlist M, Derkinderen P. A comparison between rectal and colonic biopsies to detect Lewy pathology in Parkinson's disease. Neurobiology of disease. 2012; 45:305–309. [PubMed: 21878391]

Ryter A. Relationship between ultrastructure and specific functions of macrophages. Comparative immunology, microbiology and infectious diseases. 1985; 8:119–133.

Santer RM, Baker DM. Enteric neuron numbers and sizes in Auerbach's plexus in the small and large intestine of adult and aged rats. J Auton Nerv Syst. 1988; 25:59–67. [PubMed: 3225382]

Sato K, Torihashi S, Hori M, Nasu T, Ozaki H. Phagocytotic activation of muscularis resident macrophages inhibits smooth muscle contraction in rat ileum. J Vet Med Sci. 2007; 69:1053–1060. [PubMed: 17984593]

Smith PD, Smythies LE, Shen R, Greenwell-Wild T, Gliozzi M, Wahl SM. Intestinal macrophages and response to microbial encroachment. Mucosal Immunol. 2011; 4:31–42. [PubMed: 20962772]

Streit WJ. Microglial senescence: does the brain's immune system have an expiration date? Trends Neurosci. 2006; 29:506–510. [PubMed: 16859761]

Talley NJ, O'Keefe EA, Zinsmeister AR, Melton LJ 3rd. Prevalence of gastrointestinal symptoms in the elderly: a population-based study. Gastroenterology. 1992; 102:895–901. [PubMed: 1537525]

Varin A, Gordon S. Alternative activation of macrophages: immune function and cellular biology. Immunobiology. 2009; 214:630–641. [PubMed: 19264378]

Vasina V, Barbara G, Talamonti L, Stanghellini V, Corinaldesi R, Tonini M, De Ponti F, De Giorgio R. Enteric neuroplasticity evoked by inflammation. Auton Neurosci. 2006; 126–127:264–272.

Wakabayashi K, Takahashi H. Neuropathology of autonomic nervous system in Parkinson's disease. Eur Neurol. 1997; 38(Suppl 2):2–7. [PubMed: 9387796]

Wakabayashi K, Takahashi H, Ohama E, Ikuta F. Parkinson's disease: an immunohistochemical study of Lewy body-containing neurons in the enteric nervous system. Acta Neuropathol. 1990; 79:581–583. [PubMed: 1972853]

Yu S, Liu G, Han J, Zhang C, Li Y, Xu S, Liu C, Gao Y, Yang H, Ueda K, Chan P. Extensive nuclear localization of alpha-synuclein in normal rat brain neurons revealed by a novel monoclonal antibody. Neuroscience. 2007; 145:539–555. [PubMed: 17275196]

Zhang W, Wang T, Pei Z, Miller DS, Wu X, Block ML, Wilson B, Zhou Y, Hong JS, Zhang J. Aggregated alpha-synuclein activates microglia: a process leading to disease progression in Parkinson's disease. Faseb J. 2005; 19:533–542. [PubMed: 15791003]

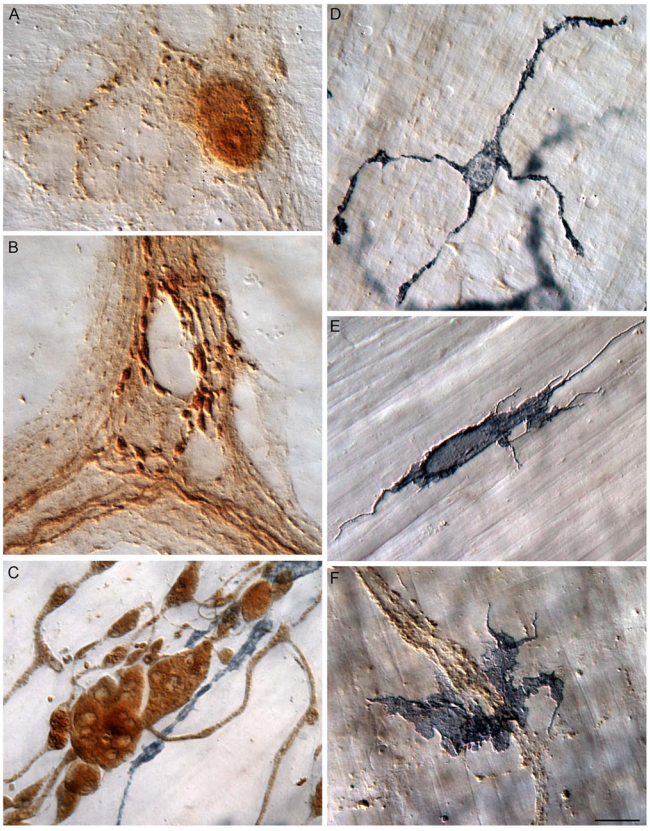

Figure 1.

Normative patterns of staining for alpha-synuclein (α-SYNC) and macrophages in the smooth muscle wall of the intestine of the gastrointestinal (GI) tract. (A) Alpha-synuclein-positive myenteric neuron illustrates that α-SYNC staining regularly stained both cytoplasm and nucleoplasm. Typically, the cytoplasm was more lightly stained, and the nucleus was more heavily stained. The nucleoli were routinely identifiable within the darkly stained nuclei. (B) The outline of unstained neurons within a myenteric ganglion are clearly silhouetted by α-SYNC+ varicosities and α-SYNC+ fibers of passage. (C) Markedly swollen axons positive for α-SYNC consisted of engorged axonal processes containing ovoid, fusiform, club-shaped, and spherical α-SYNC immunoreactive inclusions with unstained central cores which are similar to descriptions of Lewy bodies in the central and peripheral nervous system of Parkinson's patients. Macrophages (stained gray-black) immunoreactive for CD163 are clearly intertwined with the aggregated α-SYNC. (D) A macrophage immunoreactive for CD163, stellate in appearance, consisting of relatively smooth branching primary processes that radiated out from a central soma. (E) An MHCII+ macrophage illustrating the typical diverse morphology of this cell phenotype. Numerous thread-like filopodia and nodular outgrowths are clearly present protruding from the cell's parameter. (F) Often, when within close proximity to aggregated α-SYNC, MHCII+ macrophages lost their morphological definition as they spread out into large cells that would often aggregate together in large clumps. Images are from the duodenum (B, C), jejunum (A, D) and ileum (E, F) of 3- (A, B), 5- (D), and 24- (C, E, F) month-old rats. Focus stacking was used to create an extended depth of field in all panels. Scale bar in F = 10 μm for A–F.

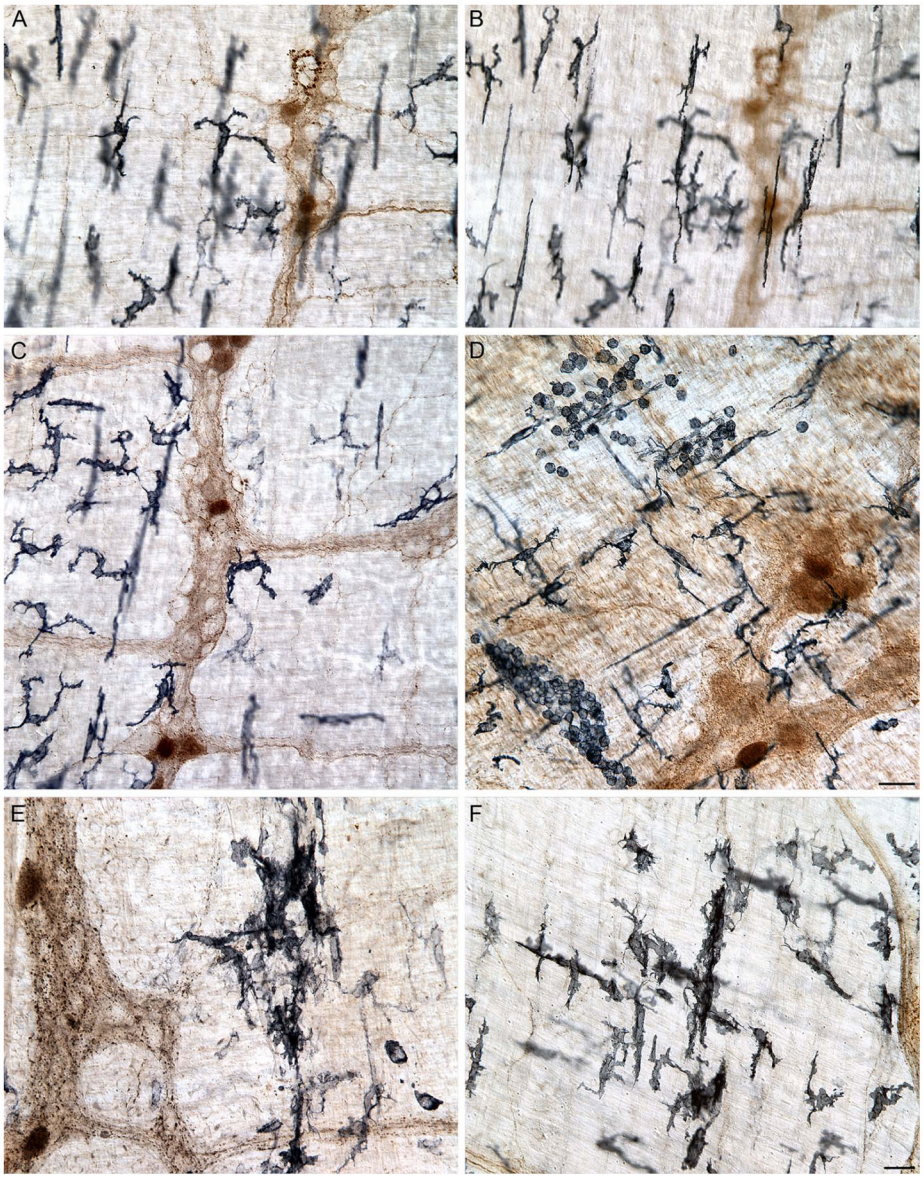

Figure 2.

Neurons, axons, and varicosities immunoreactive for α-SYNC were present in the myenteric plexus (DAB substrate; brown staining). Resident macrophages immunoreactive for major histocompatibility complex class II (MHCII; Vector SG; substrate black/dark blue cells) were located at the level of the myenteric plexus (A) and deep muscle (B). MHCII+ macrophages were unevenly distributed throughout the muscularis of the small intestine. The myenteric plexus layer is shown in Panel (C). Macrophages consisted of monocytes and amoeboid-like, bipolar, and stellate cells (D). Intensely stained clumps of MHCII+ macrophages occurred in localized and focal sites of inflammation or “hot spots” in whole mounts of the small intestine, particularly in aged animals (E, F). Images are from the jejunum (A–C, E) and ileum (D, F) of 9- (A–D) and 24- (E, F) month-old rats. Focus stacking was used to create an extended depth of field in Panels D–F. Scale bars = 25 μm in D and F (F applies to A–C, E, F).

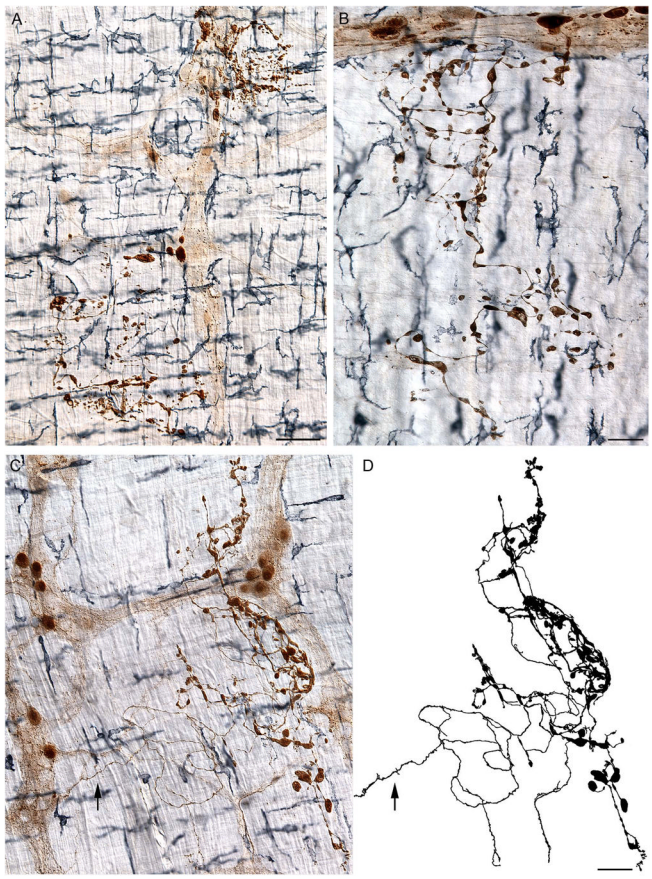

Figure 3.

There was a lack of correlation between dystrophic neurites with inclusions of α-SYNC and dense clusters of macrophages. Three separate examples are shown of α-SYNC+ markedly swollen axons at the level of the myenteric plexus in the small intestine (A–C) of aged rats double labeled for CD163. The enlarged axonal processes consisted of ovoid, fusiform, club-shaped, and spherical inclusions of α-SYNC which occurred both within (A, ganglion; B, connectives) and outside (A–C) of the plexus. A tracing (D) of the markedly swollen axon shown in Panel (C) illustrates the accumulation of misfolded α-SYNC protein at the terminal end of a strongly stained, swollen, parent axon (arrow). CD163+ macrophages were uniformly distributed around the three heteroplastic terminals without any noticeable clumping of cells. Images are from the duodenum (A, B) and ileum (C, D) of 24-month-old rats. Focus stacking was used for each image to create an extended depth of field. Scale bars = 40 μm in A and D (D applies to C, D); 75 μm in B.

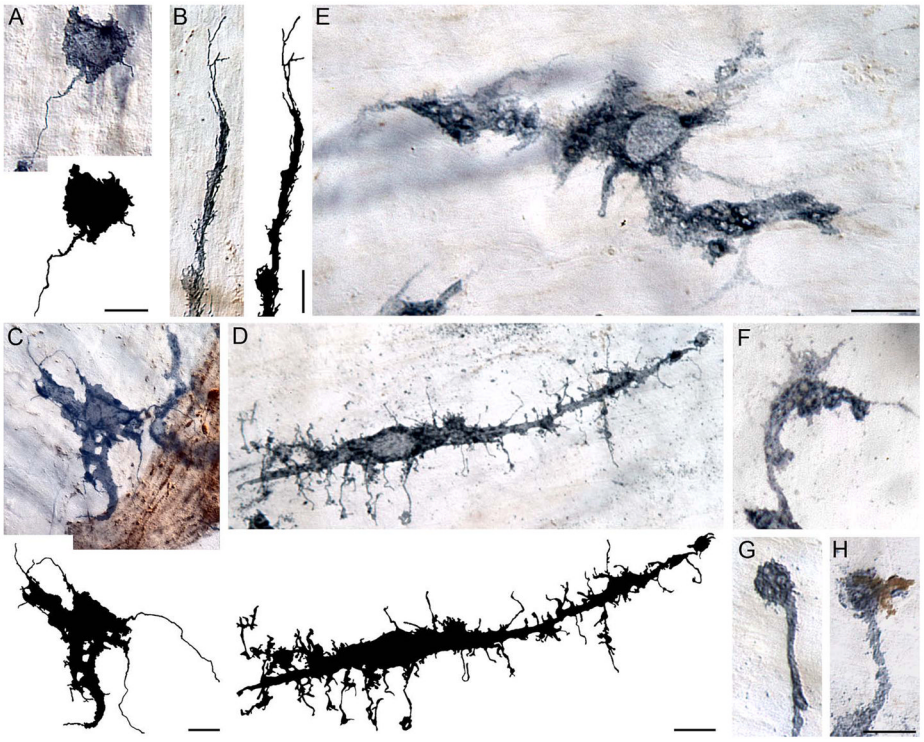

Figure 4.

The morphology of macrophages was highly variable. Macrophages often had numerous thread-like filipodia (A–C) and nodular outgrowths (D) along the cell's surface. Long, thin filipodia-like tendrils occurred both at the tips of the cell processes (B, C) and within the immediate vicinity of the cell somata (A, D); these outgrowths are highlighted in the tracings of the individual cells. Unstained vacuole-like structures were frequently observed within the cytoplasm (E) and processes (F, G) of macrophages. The vacuole-like structures were observed both unstained (G) as well as co-localized with aggregated α-SYNC (H). Images are from the duodenum (C–G) and ileum (A, B) of 9- (B, C) and 24- (A, D–H) month-old rats stained for MHCII (A–C) and CD163 (D–H). Focus stacking was used for each image to create an extended depth of field. Scale bar = 10 μm (scale bar in E applies to E–G).

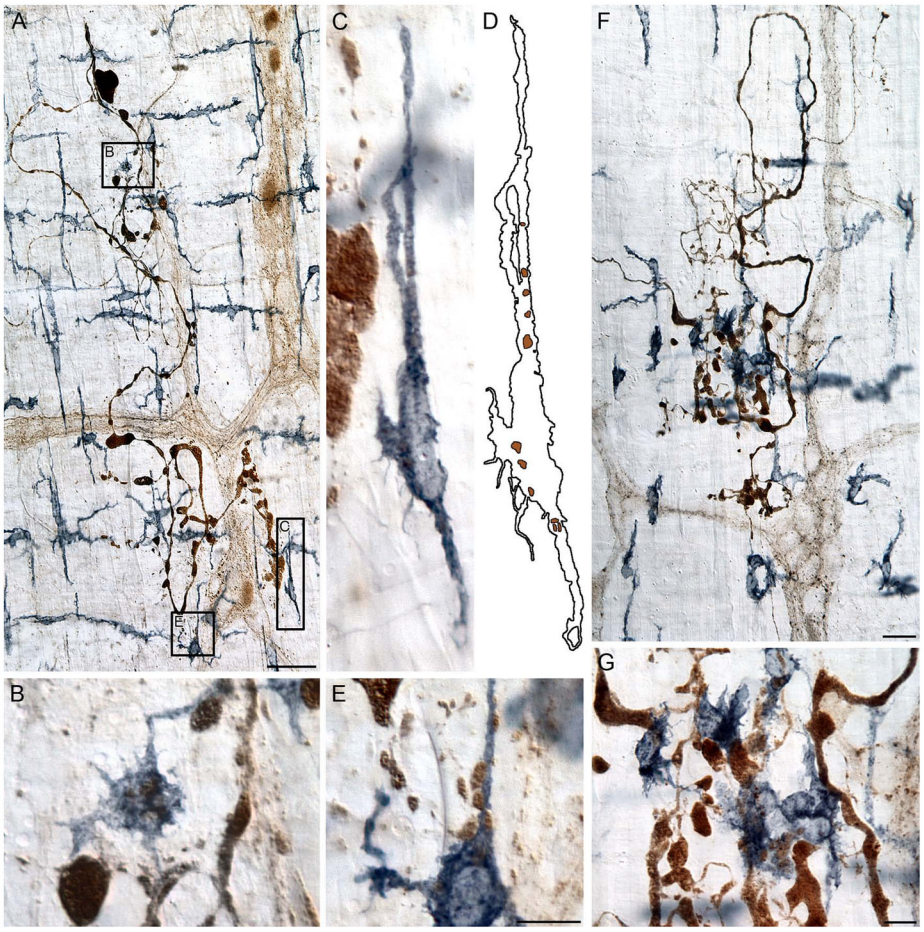

Figure 5.

The macrophage response to aggregates of α-SYNC+ material was localized to the immediate vicinity of the event. Macrophages immunoreactive for CD163 (A) and MHCII (F) are shown in close proximity to degenerating α-SYNC+ axons. The presence of aggregated α-SYNC within a macrophage (validated by scrutinizing the individual planes of focus through the z-axis and determining that the aggregate and macrophage occupied the same plane of focus) established that aggregated α-SYNC was phagocytosed by both CD163+ (B–D) and MHCII+ (G) macrophages. The outline in Panel (D) of the macrophage in Panel (C) illustrates the location of α-SYNC+ debris (brown) within the cell. Unlike CD163+ macrophages, MHCII+ macrophages often lost their morphological integrity in the presence of swollen, degenerating α-SYNC+ axons (G). These heteroplastic axons and terminal fields were from the jejunum (A–E) and ileum (F, G) of 24-month-old rats. Panels (B–E) are high power enlargements of the regions in Panel (A) outlined by the appropriately labeled boxes, and Panel (G) is a high power image of the central region of the swollen axon field shown in Panel (F). Focus stacking was used for each image to create an extended depth of field. Scale bars = 50 μm in A; 10 μm in E (applies to B–E); 25 μm in F; 10 μm in G.

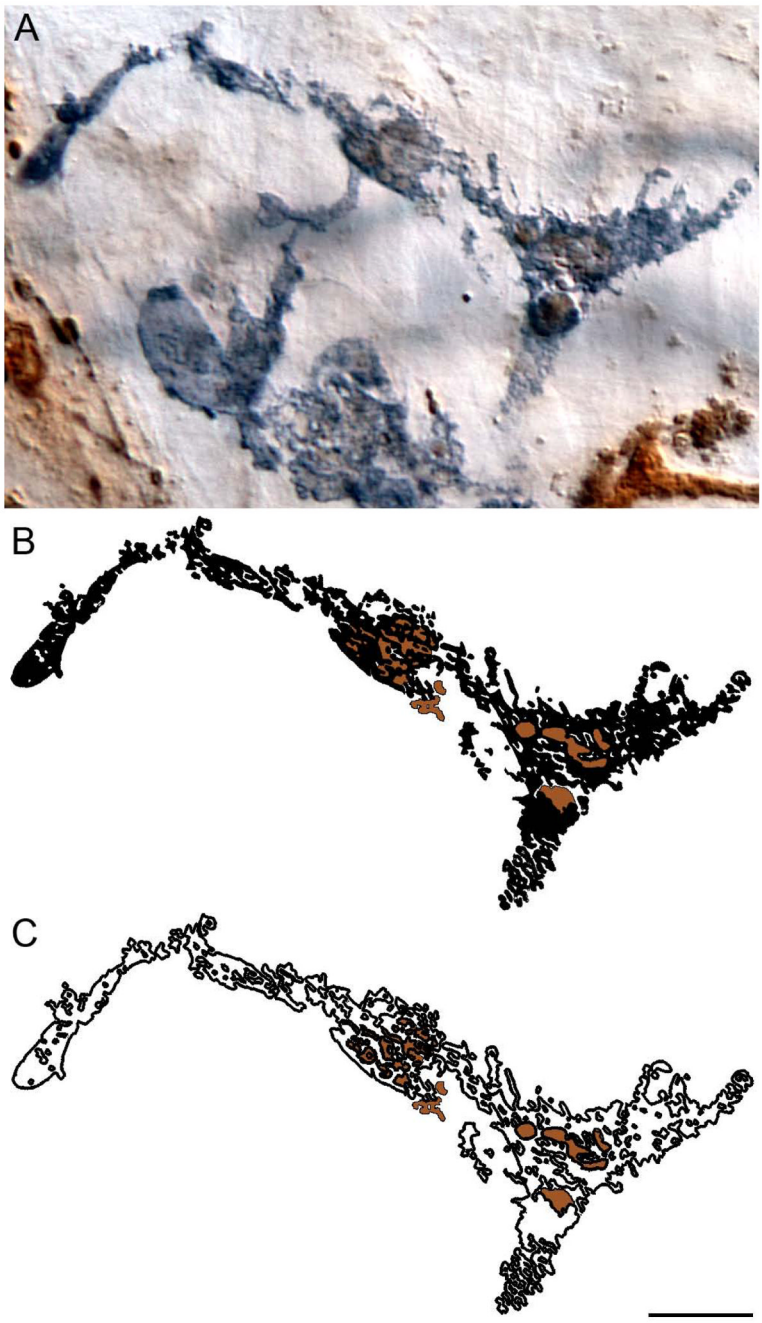

Figure 6.

Macrophages phagocytosed aggregated α-SYNC. A CD163+ macrophage in the duodenum of a 24-month-old rat contained numerous α-SYNC+ aggregates. High power examination (i.e., 100x oil objective) of the macrophage confirmed the presence of the aggregates within the same plane of focus as the macrophage, and therefore the cell's incorporation of the aggregates, consistent with phagocytosis (A). Some aggregates within the cell were round and well formed, while other aggregates were weakly stained with a flat, diffuse appearance and poorly delineated borders. Panel (B) illustrates in silhouette phagocytosed alpha-synuclein debris (dark brown) within the CD163+ macrophage (black) from panel A; this is further illustrated when only the outline of the macrophage is shown (C). Focus stacking

was used to create the extended depth of field image shown in panel A, whereas the illustrations in panels B and C were generated and validated by tracing each plane of focus throughout the z-stack. Scale bar = 10 μm in C (applies to A–C).

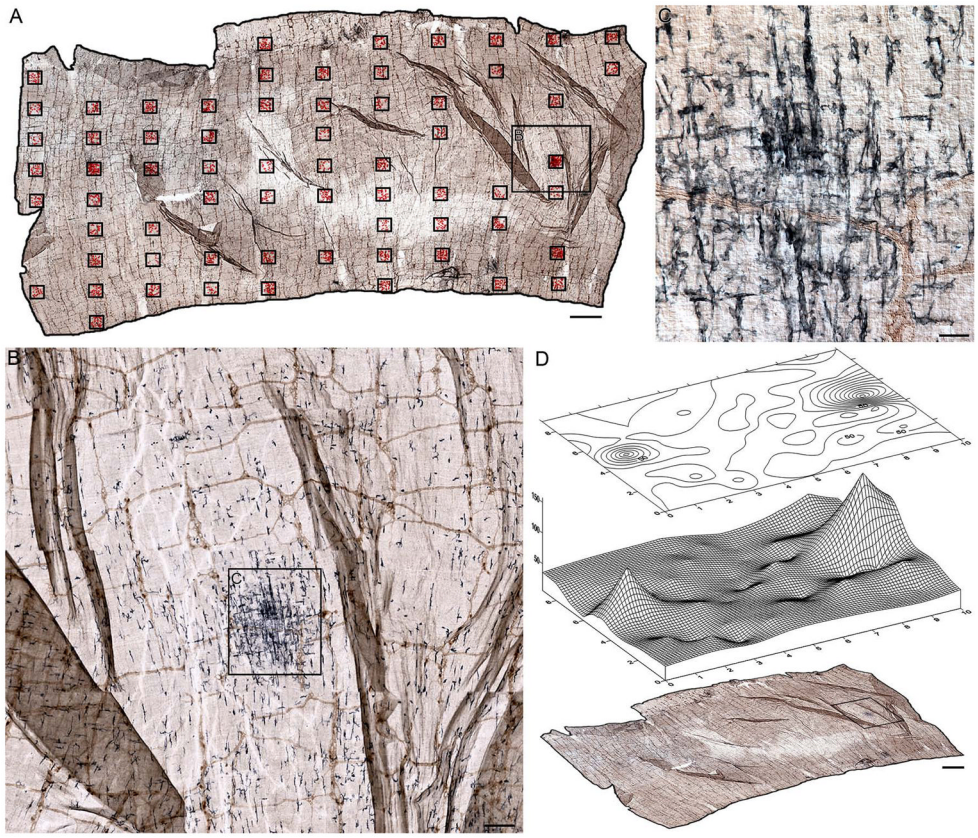

Figure 7.

Combining surveys of the whole mounts with maps of the distribution of the macrophages provided converging techniques for identifying areas of importance. Panel (A) shows a mosaic, consisting of 682 images, of a jejunal whole mount from a 9-month-old rat double labeled for α-SYNC and MHCII that was thoroughly surveyed in a systematically random fashion. Clusters of red stars superimposed on to the mosaic delineate the sites sampled, and each red star represents a single macrophage. Panels (B–D) illustrate a dense cluster of MHCII+ macrophages identified in both progressively higher power scans (B, C) and contour and surface maps of the distribution of the macrophages (D). Focus stacking was used to create an extended depth of field in panel C. Scale bars = 2 mm in A and D; 200 μm in B; 50 μm in C.

Figure 8.

Panel (A) is an ultra-high resolution mosaic, consisting of 9,546 images, of a duodenal whole mount from a 24-month-old rat double labeled for α-SYNC and CD163. A systematic scan of this whole mount identified 52 separate incidents of markedly swollen axons and large protein aggregates immunoreactive for α-SYNC. Panel (B) is an example of a single markedly swollen axon. The image was taken from the region outlined by the black box in Panel (A), and it illustrates how CD163+ macrophages were normally distributed around degenerating terminals. One pole of the heteroplastic ending shown in Panel (B) is enlarged in Panel (C) to illustrate the morphology and staining pattern of the inclusion. Focus

stacking was used to create an extended depth of field for panel C. Scale bars = 2 mm in A; 100 μm in B; 20 μm in C.

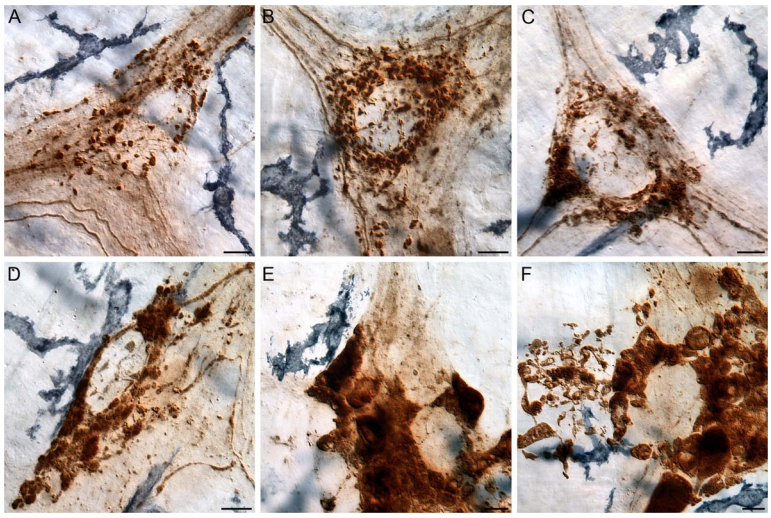

Figure 9.

Aggregated α–SYNC accumulated within the varicosities of the aged myenteric plexus. This was evidenced in adult rats by ring-like structures, which formed chains of small α-SYNC+ varicosities connected by thin axons (A) that became more pronounced in the aged rats (B–F) as a result of the accumulation of aggregated α-SYNC (C–F). In adult rats, macrophages were often in close proximity to these ring-like structures but did not contact them (A); however, macrophages accumulated within the vicinity of rings of varicosities containing aggregated alpha-synuclein (B–F). Images are from the duodenum of 5- (A) and 24- (B–F) month-old rats. Focus stacking was used for each image to create an extended depth of field. Scale bars = 10 μm in A–F.

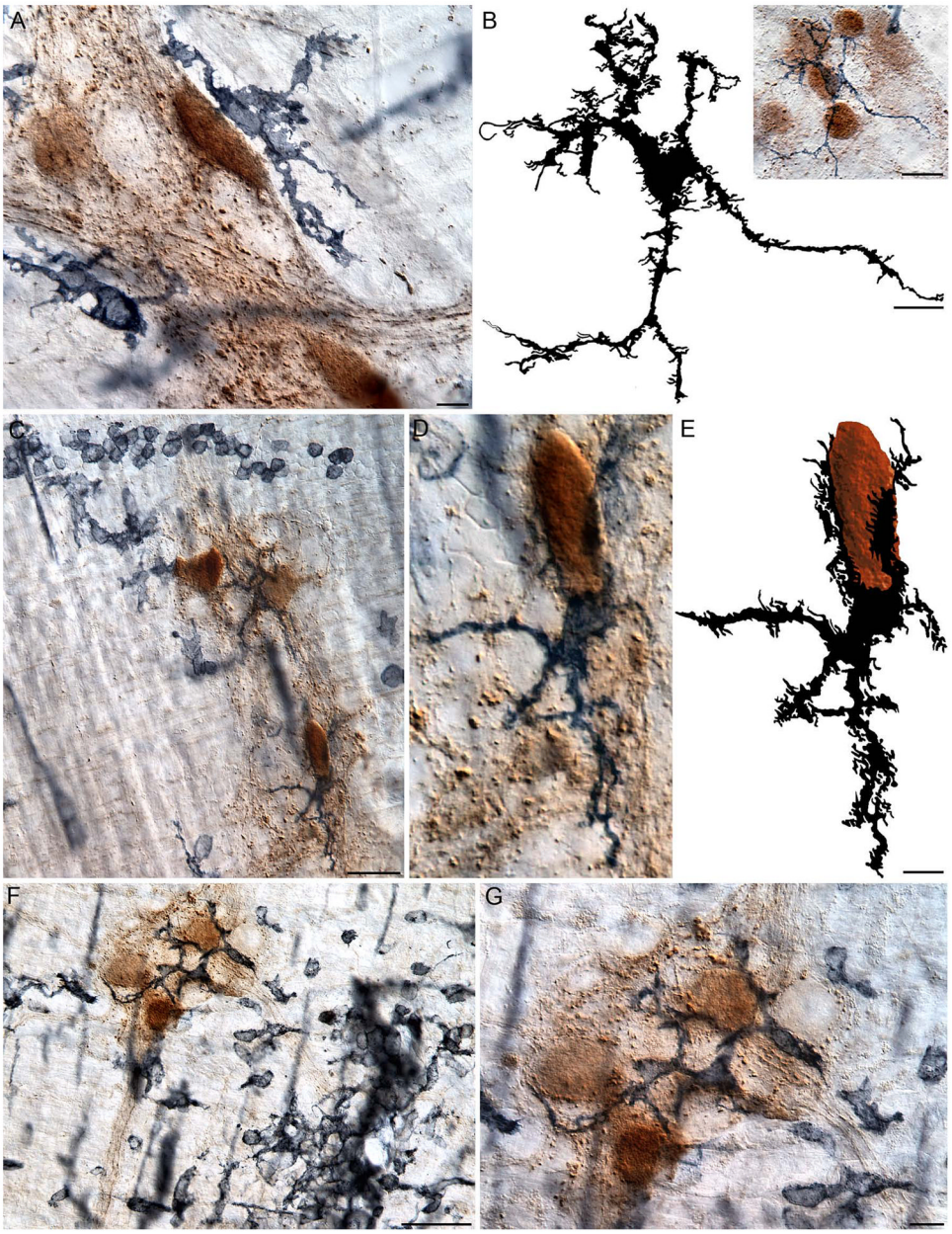

Figure 10.

In aged rats, macrophages were often observed having infiltrated ganglia that contained α-SYNC+ neurons. Typically, the soma of the macrophages would delineate the perimeter of a ganglion without crossing its borders (A), but frequently the soma and processes of macrophages invaded the ganglion and intertwined with the neurons (B–G). The traced silhouette of the macrophage shown in the inset in Panel (B) illustrates the dramatic morphology of a macrophage that is located within a ganglion containing several neurons immunoreactive for α-SYNC. Panels (C, F) are low power images illustrating monocytes and amoeboid-like cells clustered around a myenteric ganglion containing neurons darkly stained for α-SYNC. Panel (D) is a high power image of the α-SYNC+ neuron in the bottom right corner of Panel (C); one pole of the neuron is cupped by an MHCII+ macrophage. The silhouette tracing of the neuron (brown) and macrophage (black), shown in Panel (E),

illustrates the highly plastic morphology of the macrophage in relation to the neuron. Panel (G) is a high power image of the ganglion shown in Panel (F), and highlights a ganglion containing several macrophages immunoreactive for MHCII, which contact all of the α-SYNC+ neurons within the ganglion. Images are from the duodenum (A), jejunum (B), and ileum (C–D) of 24-month-old rats. Focus stacking was used for each image to create an extended depth of field. Scale bars = 10 μm in A, B, G; 20 μm in the inset in B; 40 μm in C and F; 10 μm in E (applies to D and E).